Analysis of magnetocrystalline anisotropy oscillations in Co/Pd thin films



2001 J. Phys.: Condens. Matter 13 901

(http://iopscience.iop.org/0953-8984/13/5/310)

INSTITUTE OF PHYSICS PUBLISHING JOURNAL OF PHYSICS: CONDENSED MATTER

J. Phys.: Condens. Matter **13** (2001) 901–916 www.iop.org/Journals/cm PII: S0953-8984(01)16563-X

# Analysis of magnetocrystalline anisotropy oscillations in Co/Pd thin films

**M Cinal**

Institute of Physical Chemistry of the Polish Academy of Sciences, ul. Kasprzaka 44/52, 01-224 Warszawa, Poland[1]
and
Department of Mathematics, Imperial College, 180 Queen's Gate, London SW7 2BZ, UK

Received 21 August 2000, in final form 25 October 2000

**Abstract**

The oscillations of magnetocrystalline anisotropy (MA) energy with the increasing thickness of a Pd overlayer in Co/Pd systems, obtained within a realistic five-d-band tight-binding model, are analysed thoroughly in order to determine uniquely the basic origin of the oscillations. Several techniques are applied to achieve this goal, including real- and $\boldsymbol{k}$-space breakdowns of the MA energy. The MA oscillations are shown, in a direct way, to come from pairs of majority-spin quantum-well states, confined in the Pd overlayer, and the corresponding pairs of minority-spin resonances, both occurring near the Fermi level at and in the neighbourhood of the $\overline{\Gamma}$ point of the two-dimensional Brillouin zone. The oscillatory behaviour of layer-resolved MA contributions in the Pd overlayer is also explained.

## 1. Introduction

The dependence of energy on the magnetization direction, known as magnetic anisotropy, is one of important factors in thin magnetic films. One source of this effect is shape anisotropy due to long-range dipole–dipole interaction. The other source is magnetocrystalline anisotropy (MA). The essence of MA is that the energy of an electron moving in a film depends, via spin–orbit (SO) coupling, on the direction of its spin magnetic moment with respect to the geometric structure of the film. The MA energy $E_{\mathrm{MA}}$ associated with the orientation of the film magnetization is of the second order in the SO interaction $H_{\mathrm{so}}$ and, thus, is much larger than in bulk cubic ferromagnets where $E_{\mathrm{MA}}$ comes only as the fourth-order correction to the crystal energy. The origin of this effect is the reduced symmetry of thin films, compared to bulk cubic crystals, due to the existence of surfaces and/or interfaces. Therefore, one may be tempted to assume, as is usually done in the interpretation of experimental data (see, e.g., [1–3]), that the magnetic-anisotropy energy of a multilayer system with perfect cubic lattice consists of two parts. The MA energy coming from surfaces and interfaces present in the system is the first part which is assumed not to depend on the thicknesses of metallic films forming the multilayer.

[1] Permanent address.

0953-8984/01/050901+16$30.00  

The second part, originating in the interior of the films, is linear in the film thicknesses and is attributed mainly to shape anisotropy only, though a small bulk MA contribution is also present. However, theoretical findings prove that these assumptions are only partly true since the MA energy can oscillate significantly, around an average value, with increasing film thickness. This was reported for the thickness of a ferromagnetic film (free-standing or being a part of a multilayer system) in [4–11], but no clear explanation of the MA oscillations was given there.

A recent report [12] presented calculations showing that the MA energy of (001) fcc Pd($p$)/Co($q$)/Pd($p$) slabs oscillates with the increasing number $p$ of atomic layers (AL) in the Pd overlayer. Also, in a paper published a month earlier, Szunyogh *et al* [13] reported oscillatory behaviour of MA in (001) fcc Co/Cu multilayer systems versus both Co and Cu layer thicknesses. In these two reports, for the first time, MA oscillations versus the thickness of a *non-magnetic* overlayer were predicted theoretically. Earlier, similar MA oscillations were found experimentally for a stepped (001) Co fcc surface covered with Cu overlayer of varying thickness [14]. Also, MA oscillations versus Cu thickness were reported for Cu/Co/Au(111) fcc trilayers [15]. Although, similar oscillations have not been found in experiments on Co/Pd thin films [16, 17] so far, I believe that the different behaviour of the Co/Pd and Co/Cu experimental systems can be attributed to imperfections of Co/Pd interfaces measured, especially to alloying at the interfaces and/or their roughness. This conviction is supported by the fact that a significant effect of surface quality on quantum oscillations has been found experimentally for Co/Cu stepped surfaces [18]. However, the interface imperfections are not included in the present model, similar to all previous theoretical MA approaches.

In [12], the MA oscillations in the Co/Pd systems were assumed to be induced by pairs of quantum-well (QW) states confined within the Pd overlayer, each pair being degenerate at the $\overline{\Gamma}$ point of the two-dimensional, surface, Brillouin zone (2D-BZ). This assumption was, in fact, partly based on the results to be presented only in the current paper. In [12], the majority-spin QW states, forming the pairs, were derived from bulk Pd electronic states, obtained in a two-band tight-binding (TB) model, whose three-dimensional wave-vectors were later quantized, in a simple way, in the direction perpendicular to the slab surface. This approach reproduced the MA oscillation period and related it to the extremal dimension of the bulk Pd Fermi surface. A similar relation had previously been found for oscillation periods of the exchange coupling in magnetic multilayers (see, e.g., [19, 20]).

The objective of the present paper is to *analyse* the MA oscillations versus the Pd thickness in Co/Pd systems within the full five-d-band canonical TB slab model, in a thorough and systematic way, in order to reveal the basic internal mechanism governing these oscillations. As a result, the connection between the MA oscillations and the QW state pairs, *assumed* in [12], is now *deduced directly* in the TB model. This goal is achieved by a variety of techniques in which the MA energy is broken down in various ways. The argument starts with real-space analysis of MA done either by switching off the SO interaction in the Co or Pd layers or by looking at the layer-by-layer breakdown of MA. Then, we study how states with different energies, close and far from the Fermi level, influence MA. Next, we determine the region in the 2D-BZ where the MA oscillations come from. Further, we take an even closer look, down to individual electronic states which contribute to MA. Thus, the effect of majority-spin QW states and minority-spin resonances on MA is revealed. The simplified, semi-analytical, TB model used in [12] for majority-spin QW states is given a formal justification. It is further enhanced to describe the minority-spin resonances and explain why they appear in phase with the majority-spin QW states. The semi-analytical TB model also leads to understanding of real-space oscillations of the layer MA contributions in the Pd overlayer.

The TB approach used in the present paper to treat the MA problem is, to some extent, a model calculation when compared with sophisticated *ab initio* methods. However, it should be

stressed that, despite the somewhat poorer accuracy of TB models, the previous calculations for Fe, Co, Ni surfaces and Co/Pd interfaces [6, 8] have proved that a carefully set TB model, though not fully self-consistent, is able to reproduce correctly the sign of the MA energy and its order of magnitude. Also, it was the TB model that first predicted the existence of MA oscillations in magnetic layered systems [6]. Because the TB model is simple and easy to solve numerically, even for thick films, one is able to analyse the MA problem thoroughly and efficiently. In particular, the use of the present *slab* TB model has such an advantage over a Green-function *ab initio* approach that the TB model allows one to monitor the effect on MA of *individual* quantum states.

## 2. Theory

A detailed formulation of the theory of MA for slabs in finite temperature $T$ has been given in [8]. Below, we summarize briefly the main results which will be used in the present calculations.

We consider slabs built from atomic layers of transition metals. Some atomic layers have net spin magnetic moments $\boldsymbol{M}^{(l)}$ (per atom). The moments $\boldsymbol{M}^{(l)}$ are assumed to be collinear and pointing in a direction characterized by the polar angle $\theta$ made with the slab surface normal and by an azimuthal angle $\phi$ around the normal. For a (001) fcc slab, the $z$-axis is chosen to be perpendicular to the surface while the $x$- and $y$-axes are along the axes of the square surface lattice; $\phi$ is measured from the $x$-axis. The square lattice constant is $a_{2\mathrm{d}} = a/\sqrt{2}$ where $a$ denotes the fcc lattice constant.

The spins of electrons are coupled to their orbital moments on each atom, [6,8,21] the spin–orbit coupling constant $\xi_l$ being potentially different for each layer $l$. The spin–orbit interaction $H_{\mathrm{so}}$ is treated as a perturbation and gives non-zero corrections to the thermodynamic potential $\Omega$ in even orders only [8]. In the case of a slab, unlike for bulk cubic crystals, the second-order correction $\Omega^{(2)}$ depends on the pre-set $(\theta, \phi)$-direction of the slab magnetization. The angle-dependent part of $\Omega^{(2)}/N$ is identified as the MA energy $E_{\mathrm{MA}}$ (per surface atom):

$$E_{\mathrm{MA}}(\theta, \phi) = K_1 \cos^2\theta + K_2 \sin^2\theta \cos^2\phi \tag{1}$$

where $N$ is the number of atoms in each atomic layer (equal to the number of $\boldsymbol{k}$-points in the two-dimensional BZ). The above form of the MA energy is valid for (001) and (110) fcc or bcc slabs, as studied previously [6–8, 12]. For (001) fcc slabs, $K_2 = 0$ and the anisotropy constant $K_1$ is given by the following formula [8]

$$\begin{aligned} K_1 = \Bigg[ & \frac{1}{8}Q_{1212} - \frac{1}{4}Q_{1234} + \frac{\sqrt{3}}{4}Q_{1235} + \frac{1}{8}Q_{1313} + \frac{1}{4}Q_{1324} + \frac{\sqrt{3}}{4}Q_{1325} - Q_{1414} - Q_{1423} \\ & - \frac{1}{4}Q_{2323} + \frac{1}{8}Q_{2424} + \frac{\sqrt{3}}{4}Q_{2425} + \frac{3}{8}Q_{2525} + \frac{1}{8}Q_{3434} - \frac{\sqrt{3}}{4}Q_{3435} + \frac{3}{8}Q_{3535} \Bigg] \end{aligned} \tag{2}$$

where

$$Q_{\mu_1\mu_2\mu_3\mu_4} = I^{\uparrow\uparrow}_{\mu_1\mu_2\mu_3\mu_4} - I^{\uparrow\downarrow}_{\mu_1\mu_2\mu_3\mu_4} - I^{\downarrow\uparrow}_{\mu_1\mu_2\mu_3\mu_4} + I^{\downarrow\downarrow}_{\mu_1\mu_2\mu_3\mu_4} \tag{3}$$

$$I^{\sigma'\sigma''}_{\mu_1\mu_2\mu_3\mu_4} = \mathrm{Re}\left[ J^{\sigma'\sigma''}_{\mu_1\mu_2\mu_3\mu_4} - J^{\sigma'\sigma''}_{\mu_2\mu_1\mu_3\mu_4} - J^{\sigma'\sigma''}_{\mu_1\mu_2\mu_4\mu_3} + J^{\sigma'\sigma''}_{\mu_2\mu_1\mu_4\mu_3} \right] \tag{4}$$

$$J^{\sigma'\sigma''}_{\mu_1\mu_2\mu_3\mu_4} = \frac{1}{2N}\sum_{\boldsymbol{k}}\sum_{n'n''}\frac{f\left(\epsilon_{n''\sigma''}(\boldsymbol{k})\right) - f\left(\epsilon_{n'\sigma'}(\boldsymbol{k})\right)}{\epsilon_{n''\sigma''}(\boldsymbol{k}) - \epsilon_{n'\sigma'}(\boldsymbol{k})} \times \sum_{l'}\xi_{l'}a^{\sigma''}_{n'',l'\mu_2}(\boldsymbol{k})[a^{\sigma'}_{n',l'\mu_1}(\boldsymbol{k})]^* \sum_{l''}\xi_{l''}a^{\sigma'}_{n',l''\mu_4}(\boldsymbol{k})[a^{\sigma''}_{n'',l''\mu_3}(\boldsymbol{k})]^*. \tag{5}$$

Here, $\epsilon_{n\sigma}(\boldsymbol{k})$ are eigen-energies of an electron with spin $\sigma$ and two-dimensional wave-vector $\boldsymbol{k}$ parallel to the slab surface when the spin–orbit coupling is absent. These eigen-energies and the corresponding eigenstates

$$|n\boldsymbol{k}\sigma\rangle = \sum_{l\mu} a^{\sigma}_{n,l\mu}(\boldsymbol{k})|\boldsymbol{k}l\mu\sigma\rangle \tag{6}$$

are found by diagonalizing the matrix $H^{\sigma}_{l\mu,l'\nu}(\boldsymbol{k}) = \langle \boldsymbol{k}l\mu\sigma|H|\boldsymbol{k}l'\nu\sigma\rangle$ of the slab Hamiltonian $H$ in the in-plane basis $|\boldsymbol{k}l\mu\sigma\rangle$. Each basis state $|\boldsymbol{k}l\mu\sigma\rangle$ is a two-dimensional Bloch state, in atomic layer $l$, formed from atomic orbitals $\mu$ on each site (cf. [6–8]). The Hamiltonian matrix is calculated in the two-centre approximation [22] and is assumed to depend on the spin $\sigma$ only through the exchange term $\frac{1}{2}s(\sigma)\Delta^{(l)}_{\rm ex}\delta_{\mu\nu}\delta_{ll'}$ where $s(\uparrow) = -1$, $s(\downarrow) = 1$ and $\Delta^{(l)}_{\rm ex}$ is a layer-dependent exchange splitting. In the present calculations we use five d-orbitals: $xy$, $yz$, $zx$, $x^2 - y^2$, $3z^2 - r^2$ which are numbered in equation (2) as 1, 2, 3, 4 and 5, respectively. The canonical two-centre TB parameters are adopted for the d-orbitals in the Hamiltonian matrix elements between first- and second-nearest-neighbours. [6, 8, 23, 24] On-site layer-dependent potentials are determined self-consistently in order to obtain the correct magnetic moments in Co layers and d-electron occupations in Pd layers. This also sets the position of the Fermi energy $\epsilon_{\rm F}$ within the d band. The Co magnetic moments and Pd d-electron occupations are taken from *ab initio* calculations and thus are not calculated self-consistently. The present TB model cannot be fully self-consistent due to the fact that only d-orbitals are taken into account. It is possible to restrict the TB model to d states only because the Fermi level, whose position is important for MA (cf. section 3.2), lies within the d-band both in Co and Pd. The SO coupling constants $\xi_l$, present in equation (5), are chosen as $\xi_{\rm Co} = 0.085$eV in Co layers and $\xi_{\rm Pd} = 0.23$eV in Pd layers [8, 12]. Other details of the applied TB model can be found in [8].

Expressions (2)–(5) for the MA constant $K_1$ depend on temperature $T$ only through the Fermi–Dirac function $f(\epsilon) = \{1 + \exp[\beta(\epsilon - \epsilon_{\rm F})]\}^{-1}$ where $\beta = k_{\rm B}T$, $\epsilon_{\rm F}$ is the Fermi energy, and $k_{\rm B}$ is the Boltzmann constant. Thus, the present approach takes no account of the temperature dependence of the magnetization. Consequently, the temperature dependence of the average value of the MA energy is not correctly described. However, one real effect of finite temperature *is* included. This is the reduction in amplitude of oscillations of the MA energy about its mean value, as a function of film thickness, due to thermal smearing [8]. A very useful feature of working at finite $T$ is that one needs fewer $\boldsymbol{k}$-points in numerical calculations of the MA constants than at $T = 0$; cf. [6, 8].

The anisotropy constant $K_1$ given by the formulae (2)–(5) is a sum over $\boldsymbol{k}$-points from the whole 2D-BZ:

$$K_1 = \frac{1}{N}\sum_{\boldsymbol{k}}\tilde{b}_1(\boldsymbol{k}). \tag{7}$$

The anisotropy constant $K_1$, as well as $\Omega^{(2)}$, can also be broken down into individual atomic layer contributions $K^{(l)}_1$ (cf. [8, 9, 13]). It is shown in [8] that to calculate individual $K^{(l)}_1$ we can still use the formulae (2)–(4) *provided that* $J^{\sigma'\sigma''}_{\mu_1\mu_2\mu_3\mu_4}$ is replaced with

$$J^{\sigma\sigma' l}_{\mu_1\mu_2\mu_3\mu_4} = -\frac{1}{N}\sum_{\boldsymbol{k}}\sum_{n_1 n_2 n_3} S\left[\epsilon_{n_1\sigma}(\boldsymbol{k}), \epsilon_{n_2\sigma'}(\boldsymbol{k}), \epsilon_{n_3\sigma}(\boldsymbol{k})\right]\sum_{\mu} a^{\sigma}_{n_1,l\mu}(\boldsymbol{k})[a^{\sigma}_{n_3,l\mu}(\boldsymbol{k})]^* \times \sum_{l'}\xi_{l'}a^{\sigma'}_{n_2,l'\mu_2}(\boldsymbol{k})[a^{\sigma}_{n_1,l'\mu_1}(\boldsymbol{k})]^*\sum_{l''}\xi_{l''}a^{\sigma}_{n_3,l''\mu_4}(\boldsymbol{k})[a^{\sigma'}_{n_2,l''\mu_3}(\boldsymbol{k})]^* \tag{8}$$

where

$$S(\epsilon_1,\epsilon_2,\epsilon_3) = \frac{k_{\mathrm{B}}T}{\epsilon_3-\epsilon_2}\left[\frac{L(\epsilon_3)-L(\epsilon_1)}{\epsilon_3-\epsilon_1} - \frac{L(\epsilon_2)-L(\epsilon_1)}{\epsilon_2-\epsilon_1}\right] \tag{9}$$

$$L(\epsilon) = \log\left(1+\exp[\beta(\epsilon_{\mathrm{F}}-\epsilon)]\right). \tag{10}$$

It is obvious that the dipole–dipole interaction energy of the investigated Co/Pd film is independent of the non-magnetic Pd overlayer thickness and as such is neglected. Therefore, only the MA contribution to the total magnetic-anisotropy energy is considered in the present paper.

## 3. Results and analysis

As reported earlier [12], the anisotropy constant $K_1$ of Pd($p$)/Co(16)/Pd($p$) (001) fcc structures calculated with the formulae (2)–(5) in the five-d-band TB model exhibits remarkable oscillations, of a period of around 6 AL, when the Pd overlayer thickness $p$ is varied; see figure 1. Below we will reveal, step by step, the physical origin of the MA oscillations.

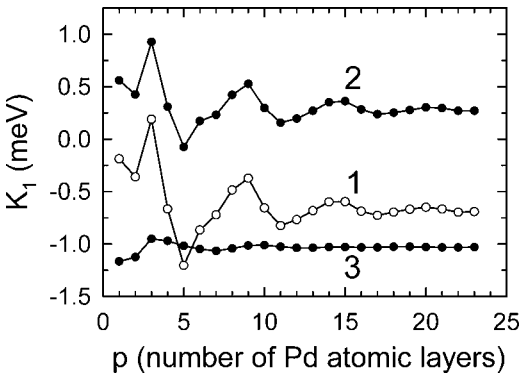


**Figure 1.** MA constant $K_1$ against Pd overlayer thickness $p$ for a (001) fcc Pd($p$)/Co(16)/Pd($p$) slab (line 1) compared with fictitious $K_1$ calculated with $\xi_{\mathrm{Co}} = 0$ (line 2) or $\xi_{\mathrm{Pd}} = 0$ (line 3); $T = 300$ K.

### *3.1. Analysis of MA oscillations in real space*

The oscillations of $K_1$ versus the Pd thickness $p$ are surprising, especially in view of the fact that, apart from the three Pd layers closest to the Co/Pd interface, which are only slightly magnetized, the rest of the Pd overlayer is virtually non-magnetic (cf. [8]). For a paramagnetic free-standing slab, $K_1$ always vanishes since for zero net magnetization the slab energy cannot depend on the magnetization direction. This is also true in our formalism where the quantities $I^{\sigma'\sigma''}_{\mu_1\mu_2\mu_3\mu_4}$ entering the expression (3) are the same for all spin pairs $\sigma'\sigma''$ when the (paramagnetic) electronic structure is identical for both spins. At this point, one could argue that it is a

periodic change of the electronic structure of the ferromagnetic Co substrate, induced near the Co/Pd interface by varying the thickness of the Pd overlayer, that leads, through the SO coupling on Co atoms, to the oscillations of $K_1$. However, a direct check shows that the opposite is true. In figure 1, we show $K_1$ calculated with either $\xi_{\mathrm{Co}}$ or $\xi_{\mathrm{Pd}}$ set to zero. When $\xi_{\mathrm{Co}}$ is set to zero the oscillatory part of $K_1$ remains largely unchanged (though the mean value of $K_1$ is shifted) while with $\xi_{\mathrm{Pd}} = 0$ (and $\xi_{\mathrm{Co}}$ unchanged) the oscillations of $K_1$ are almost wiped out. These results prove clearly that the MA oscillations originate almost entirely within the Pd overlayer. An important factor that facilitates this simple picture to emerge is the large value of the ratio $\xi^2_{\mathrm{Pd}}/\xi^2_{\mathrm{Co}} = 7.32$ while $K_1$ is a quadratic form of $\xi_{\mathrm{Co}}$ and $\xi_{\mathrm{Pd}}$; cf. equation (5).

The conclusion about the dominant role of the Pd overlayer in the actual Pd($p$)/Co(16)/Pd($p$) slabs studied here is confirmed by examining layer contributions $K_1^{(l)}$ to the MA constant. Figure 2 shows these contributions for different Pd thicknesses $p = 5, 6, 7, 8, 9, 10$ and 11. We find out that, for each $p$, the contribution $K_1^{(l)}$ oscillates versus the atomic-layer position $l$ in the Pd overlayer with roughly the same period of around 6 AL, strikingly similar to the period of the oscillations of the total $K_1$ as a function of $p$. Also, in the Pd overlayer each $K_1^{(l)}$ changes with increasing $p$ in a similar, oscillatory, manner to the whole $K_1$, with minima at $p = 5$ and $p = 11$ and a maximum at $p = 9$. On the other hand, the variations of $K_1^{(l)}$ versus $p$ are much smaller in the Co layers.

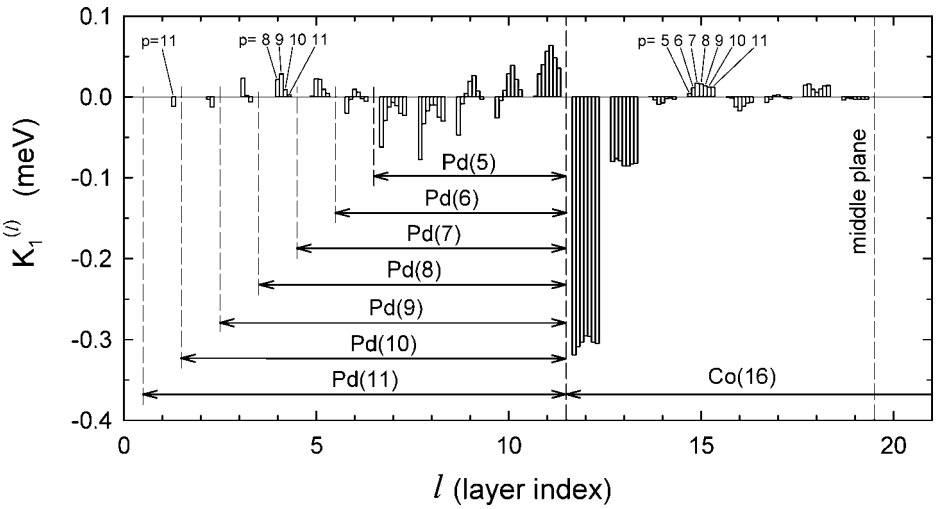


**Figure 2.** Layer contributions $K_1^{(l)}$ to MA constant in a (001) fcc Pd($p$)/Co(16)/Pd($p$) slab for $p = 5, 6, 7, 8, 9, 10, 11$. The different slabs presented are so aligned that the interface Pd layer is at $l = 11$ for every slab. For each $l$ there are up to seven subbars, each of which represents $K_1^{(l)}$ for a different Pd thickness $p$ so that in the composite bar for this $l$ the rightmost subbar corresponds to $p = 11$ and $p$ decreases by 1 with each new subbar when moving across the bar to the left. This assignment is marked explicitely for $l = 1$, 4, and 15. The contributions $K_1^{(l)}$ are shown in one half of each slab only and are symmetrical in the other half.

### *3.2. Role of Fermi level*

The structure of the expressions (5) for MA constants suggests that MA oscillations arise from the changes of electronic structure around the Fermi energy $\epsilon_{\mathrm{F}}$ as was already noted in [4]. Damping of MA oscillations with increase of $T$ (cf. [8]) also indicates they are due to states at $\epsilon_{\mathrm{F}}$. This can be demonstrated directly in the present case by plotting the contribution

$K_1^{\mathrm{F}}(\Delta\epsilon)$ to the total anisotropy constant $K_1$ coming from states $|n'\sigma'\boldsymbol{k}\rangle$, $|n''\sigma''\boldsymbol{k}\rangle$ appearing in the expression (5) which have energies $\epsilon_{n'\sigma'}(\boldsymbol{k})$, $\epsilon_{n''\sigma''}(\boldsymbol{k})$ lying within a $[\epsilon_{\mathrm{F}} - \Delta\epsilon, \epsilon_{\mathrm{F}} + \Delta\epsilon]$ interval. It is clearly seen in figure 3 that for $\Delta\epsilon = 0.5$ eV the contribution $K_1^{\mathrm{F}}$ exhibits 6-AL-period oscillations which follow closely the oscillations of the total $K_1$. The remaining MA contributions: $K_1^{\mathrm{nF}}$ and $K_1 - K_1^{\mathrm{F}} - K_1^{\mathrm{nF}} \equiv K_1^{\mathrm{FnF}}$, corresponding, respectively, to two and one of the states $|n'\sigma'\boldsymbol{k}\rangle$, $|n''\sigma''\boldsymbol{k}\rangle$ lying outside the $[\epsilon_{\mathrm{F}} - \Delta\epsilon, \epsilon_{\mathrm{F}} + \Delta\epsilon]$ interval, are more or less constant for $p \geqslant 5$.

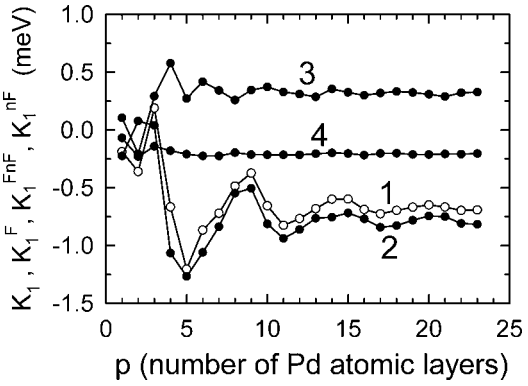


**Figure 3.** MA constant $K_1$ against Pd overlayer thickness $p$ for a (001) fcc Pd($p$)/Co(16)/Pd($p$) slab (line 1) compared with $K_1^{\mathrm{F}}$ (line 2), $K_1^{\mathrm{FnF}}$ (line 3), and $K_1^{\mathrm{nF}}$ (line 4) calculated according to formulae (2-5) but using only those states $|n'\sigma'\boldsymbol{k}\rangle$, $|n''\sigma''\boldsymbol{k}\rangle$ whose energies $\epsilon_{n'\sigma'}(\boldsymbol{k})$, $\epsilon_{n''\sigma''}(\boldsymbol{k})$ are such that they both lie within the $[\epsilon_{\mathrm{F}} - \Delta\epsilon, \epsilon_{\mathrm{F}} + \Delta\epsilon]$ interval or only one of them does or none does, respectively; $\Delta\epsilon = 0.5$ meV, $T = 300$ K.

### *3.3. Breakdown of MA energy in $\boldsymbol{k}$-space*

The contributions $\tilde{b}_1(\boldsymbol{k})$ to the MA constant $K_1$ come from the whole 2D-BZ (cf. figure 8 in [8]). To see whether the oscillations of $K_1$ versus the Pd thickness $p$ can be associated with a certain region in the 2D-BZ we plot the oscillatory part of $\tilde{b}_1(\boldsymbol{k})$ defined as

$$\tilde{b}_1^{\mathrm{osc}}(\boldsymbol{k}) = \tilde{b}_1(\boldsymbol{k}) - \tilde{b}_1^{\mathrm{av}}(\boldsymbol{k}). \tag{11}$$

Here, $\tilde{b}_1^{\mathrm{av}}(\boldsymbol{k})$ is the average of $\tilde{b}_1(\boldsymbol{k})$ with respect to $p$ at a given $\boldsymbol{k}$-point (or, equivalently, $\tilde{b}_1^{\mathrm{av}}(\boldsymbol{k}) = \lim_{p\to\infty} \tilde{b}_1(\boldsymbol{k})$). In these calculations, $\tilde{b}_1^{\mathrm{av}}(\boldsymbol{k})$ is approximated by

$$\tilde{b}_1^{\mathrm{av}}(\boldsymbol{k}) = \frac{1}{p_2 - p_1 + 1} \sum_{p=p_1}^{p_2} \tilde{b}_1(\boldsymbol{k}) \tag{12}$$

where $p_1 = 12$, $p_2 = 23$. Figure 4 shows the plots of $\tilde{b}_1^{\mathrm{osc}}(\boldsymbol{k})$ for $p = 5, 7, 9, 11$. As can be seen, when the Pd overlayer thickness $p$ is varied the most significant changes of the $\tilde{b}_1^{\mathrm{osc}}(\boldsymbol{k})$ distribution take place in the region $\Omega_\Gamma = \{\boldsymbol{k} : |k_i| \leqslant \frac{1}{4}\pi/a_{2\mathrm{d}},\ i = x, y\}$ around $\boldsymbol{k} = 0$, i.e., the $\overline{\Gamma}$ point. Indeed, for $p = 5$ and $p = 11$ (i.e., at the minima of $K_1$; cf. figure 1), $\tilde{b}_1^{\mathrm{osc}}(\boldsymbol{k})$ is large and negative in $\Omega_\Gamma$, while $\tilde{b}_1^{\mathrm{osc}}(\boldsymbol{k})$ is positive in $\Omega_\Gamma$ for $p = 7$ and $p = 9$. Some less significant variations of $\tilde{b}_1^{\mathrm{osc}}(\boldsymbol{k})$ versus $p$ are also observed in the region $\Omega_M = \{\boldsymbol{k} : \frac{3}{4}\pi/a_{2\mathrm{d}} \leqslant |k_i| \leqslant \pi/a_{2\mathrm{d}},\ i = x, y\}$ while $\tilde{b}_1^{\mathrm{osc}}(\boldsymbol{k}) \approx 0$ in the rest of the 2D-BZ where $\tilde{b}_1(\boldsymbol{k})$ remains almost unchanged. However, when we compare the parts $K_1(\Omega_\Gamma)$ and $K_1(\Omega_M)$ of the total MA constant $K_1$, coming from the regions $\Omega_\Gamma$ and $\Omega_M$ respectively, we can conclude definitely that the 6-AL-period oscillations of $K_1$ originate in the region $\Omega_\Gamma$.

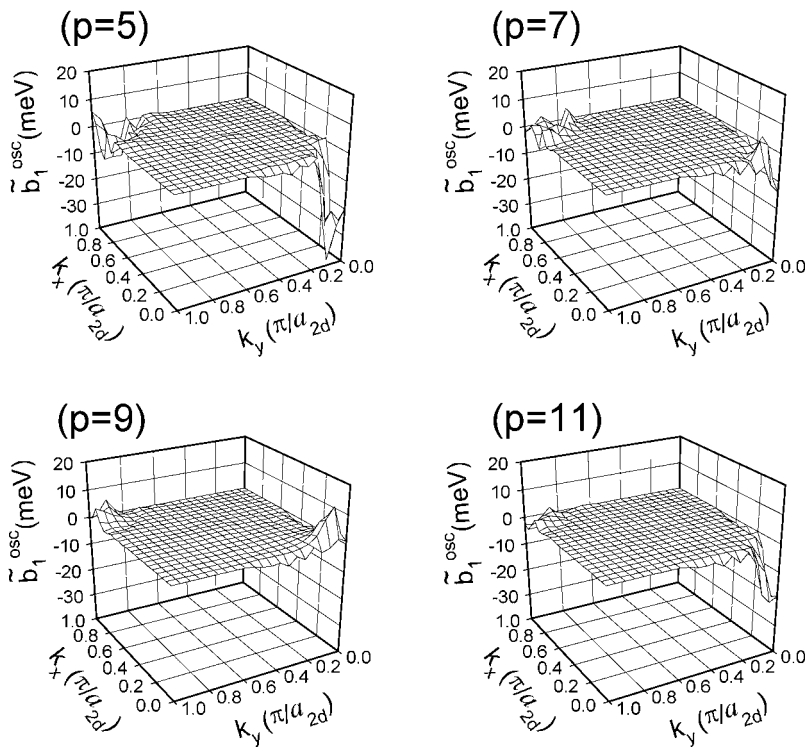


**Figure 4.** Oscillatory part $\tilde{b}_1^{\mathrm{osc}}(\boldsymbol{k})$ of the contributions $\tilde{b}_1(\boldsymbol{k})$ to MA constant $K_1$ in 1/4 of the 2D-BZ for a (001) fcc Pd($p$)/Co(16)/Pd($p$) slab with $p = 5$, $p = 7$, $p = 9$, and $p = 11$ at $T = 300$ K; cf. equations (7), (11) and (12); $a_{2\mathrm{d}}$ is the constant of the (001) fcc surface square lattice.

### *3.4. Effect of quantum-well states and resonances on MA: unique identification*

As shown in [12], all spin-pair contributions $K_1^{\sigma\sigma'}$ to the MA constant $K_1 = \sum_{\sigma\sigma'} K_1^{\sigma\sigma'}$ (cf. equations (2)–(5)) oscillate versus the Pd thickness $p$ similarly to the total $K_1$ though the oscillations of $K_1^{\uparrow\downarrow} = K_1^{\downarrow\uparrow}$ are of the opposite sign due to different signs in equation (3). The oscillations of $K_1^{\uparrow\uparrow}$ and $K_1^{\uparrow\downarrow} = K_1^{\downarrow\uparrow}$ involving up-spin electrons are more pronounced than those of $K_1^{\downarrow\downarrow}$ due to down-spin electrons only. However, when the various spin-pair contributions are summed they cancel to a large extent and the resultant sum $K_1$ has much smaller oscillations than any of the contributing terms. This implies that electrons of both spins are important for the investigated MA oscillations.

The majority-spin energies are shown near the Fermi energy $\epsilon_{\mathrm{F}}$ along the $k_y = 2k_x$ line in the $\Omega_{\overline{\Gamma}}$ region for $p = 5$, 7, 9 and 11 in figure 5. Near $\epsilon_{\mathrm{F}}$ and above, the electron states come in pairs. For each pair, the two component states are degenerate at the $\overline{\Gamma}$ point. Energies of these pairs move upwards, towards the top of the majority-spin d band, when the Pd overlayer thickness $p$ increases. For $p = 5$ and $p = 11$ there exists a pair for which the energies $\epsilon_m^+$, $\epsilon_m^-$ ($\epsilon_m^+ \geqslant \epsilon_m^-$; where $m$ is a *pair* index) of states forming it embrace the Fermi energy $\epsilon_{\mathrm{F}}$ in most of the $\Omega_{\overline{\Gamma}}$ region so that the pair gives a large contribution to $K_1^{\uparrow\uparrow}$ according to equation (5). On the other hand, for $p = 7$ and $p = 9$ the pair energies $\epsilon_m^+$, $\epsilon_m^-$ embrace $\epsilon_{\mathrm{F}}$ only in this part of $\Omega_{\overline{\Gamma}}$ where $\epsilon_m^+ - \epsilon_m^-$ is large so that the pair contribution is much smaller than for $p = 5$

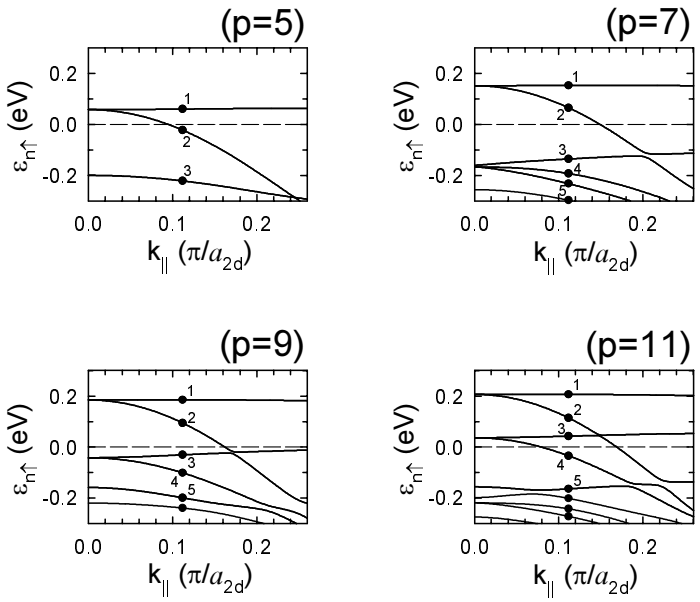


**Figure 5.** Majority-spin (up-spin) $z$-even energy bands in a (001) fcc Pd($p$)/Co(16)/Pd($p$) slab near the $\overline{\Gamma}$ point along the $k_y = 2k_x$ line for different Pd thicknesses: $p = 5$, $p = 7$, $p = 9$, and $p = 11$. $k_{||}$ is the distance $\sqrt{k_x^2 + k_y^2}$ from the $\overline{\Gamma}$ point. The energies at $\boldsymbol{k} = (0.05, 0.1)\pi/a_{2d}$ (corresponding to $k_{||} = 0.112\pi/a_{2d}$) are marked with dots (•) and labelled with the quantum number $n$ which increases with the *decreasing* state energy $\epsilon_{n\sigma}(\boldsymbol{k})$ for $\sigma = \uparrow$ so that $n = 1$ denotes the highest-energy state. The horizontal dashed line represents the Fermi energy $\epsilon_F = 0$. The majority-spin energies are identical (extremely close to each other) for $z$-even and $z$-odd states in the energy regime shown.

or 11. This mechanism is illustrated in figure 6 where the contributions $\tilde{b}^{\uparrow\uparrow}_{n'n''}(\boldsymbol{k})$ to

$$K_1^{\uparrow\uparrow} = \frac{1}{N}\sum_{\boldsymbol{k}}\sum_{n'n''}\tilde{b}^{\uparrow\uparrow}_{n'n''}(\boldsymbol{k}) \tag{13}$$

(cf. equations (2)–(5)) from all 25 doublets formed from five highest up-spin d-band quantum states $|n'\boldsymbol{k}\uparrow\rangle$, $|n''\boldsymbol{k}\uparrow\rangle$ at $\boldsymbol{k} = (0.05, 0.1)\pi/a_{2d}$ are plotted for $p = 5$, 7, 9 and 11. The contributions $\tilde{b}^{\uparrow\uparrow}_{n'n''}(\boldsymbol{k})$ shown in figure 6 are large only when the states $|n'\boldsymbol{k}\uparrow\rangle$ and $|n''\boldsymbol{k}\uparrow\rangle$ form a pair of the kind described above, and the condition $\epsilon_{n'\uparrow}(\boldsymbol{k}) < \epsilon_F < \epsilon_{n''\uparrow}(\boldsymbol{k})$ (or $\epsilon_{n''\uparrow}(\boldsymbol{k}) < \epsilon_F < \epsilon_{n'\uparrow}(\boldsymbol{k})$) is satisfied. This takes place for $p = 5$ and $p = 11$. So, every time the energy of such a pair crosses the Fermi energy at the $\overline{\Gamma}$ point when the Pd thickness $p$ increases, a downturn in $K_1^{\uparrow\uparrow}$ occurs. This happens for $p = 5$, 11, 17, 22 and so on, i.e. repeats with a period close to 6 AL.

The majority-spin, up-spin, states forming the pairs are almost perfectly confined in the Pd overlayer since the Fermi energy $\epsilon_F$ lies above the top of the Co d band for majority spin. These are QW states. The existence of d-like QW states near the Fermi level on Pd overlayers on the Co substrate was confirmed in experiment [25]. We find that the amplitudes $a^{\uparrow}_{n,l\mu}$ of these states oscillate versus $l$ with a period close to two. However, the corresponding electron probabilities $|a^{\uparrow}_{n,l\mu}|^2$ have much longer periods which depend on the state energy. For the states close to the Fermi energy, the period is around 6 AL (cf. figure 7).

For minority spin, the electronic structure near the Fermi energy is more complex than for majority spin. Many of the minority-spin states form the characteristic pairs of states

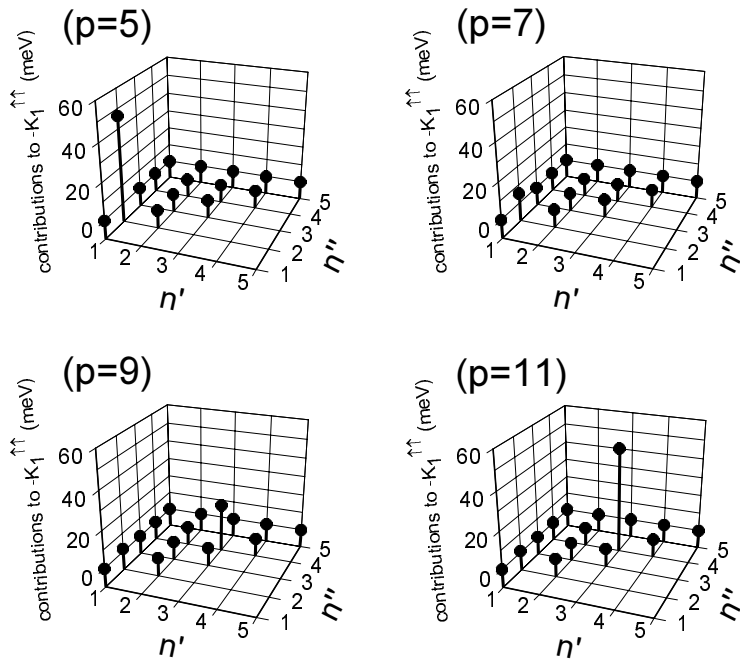


**Figure 6.** Contributions $-\tilde{b}^{\uparrow\uparrow}_{n'n''}(\boldsymbol{k})$ to $-K_1^{\uparrow\uparrow}$ from individual pairs of $z$-even quantum states $|n'\boldsymbol{k}\uparrow\rangle$, $|n''\boldsymbol{k}\uparrow\rangle$ at $\boldsymbol{k} = (0.05, 0.1)\pi/a_{2\mathrm{d}}$ in a (001) fcc Pd($p$)/Co(16)/Pd($p$) slab for $p = 5$, $p = 7$, $p = 9$, and $p = 11$; cf. equation (13); $T = 300$ K. The quantum number $n$ (i.e., $n'$ or $n''$) increases according to the *decreasing* state energy so that $n = 1$ corresponds the highest-energy $z$-even majority-spin state at the chosen $\boldsymbol{k}$. The energies of the quantum states involved here are marked with dots (•) in figure 5. For the sake of clarity, the contributions $-\tilde{b}^{\uparrow\uparrow}_{n'n''}(\boldsymbol{k})$, instead of $\tilde{b}^{\uparrow\uparrow}_{n'n''}(\boldsymbol{k})$, with $n' \leqslant n''$ only, are shown. For $n' \geqslant n''$, $-\tilde{b}^{\uparrow\uparrow}_{n'n''}(\boldsymbol{k}) = -\tilde{b}^{\uparrow\uparrow}_{n''n'}(\boldsymbol{k})$ according to equations (2)–(5) and (13). Contributions $\tilde{b}^{\uparrow\uparrow}_{n'n''}(\boldsymbol{k})$ from pairs of $z$-odd states $|n'\boldsymbol{k}\uparrow\rangle$, $|n''\boldsymbol{k}\uparrow\rangle$ are (almost) identical with the corresponding contributions from $z$-even states in the $(n', n'')$ range shown while $\tilde{b}^{\uparrow\uparrow}_{n'n''}(\boldsymbol{k})$ are significantly smaller when the states $|n'\boldsymbol{k}\uparrow\rangle$ are of different symmetry than $|n''\boldsymbol{k}\uparrow\rangle$ under the $z \to -z$ transformation.

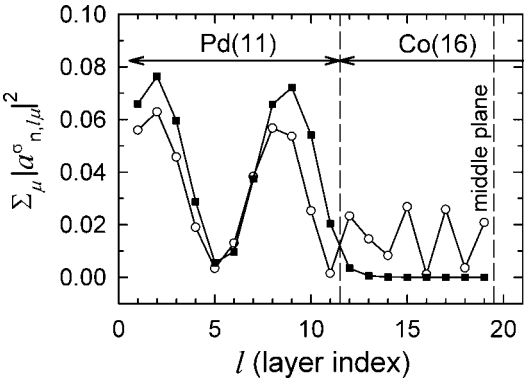


**Figure 7.** Layer electron probability $\sum_{\mu=1}^{5} |a^{\uparrow}_{n,l\mu}(\boldsymbol{k})|^2$ for the majority-spin (squares) $z$-even quantum-well state $|n\boldsymbol{k}\uparrow\rangle$, $\boldsymbol{k} = (0.05, 0.1)\pi/a_{2\mathrm{d}}$, $n = 3$, with $\epsilon_{n\uparrow}(\boldsymbol{k}) - \epsilon_{\mathrm{F}} = 0.0427$ eV (cf. figure 5 for $k_{||} = 0.112\pi/a_{2\mathrm{d}}$) and for the minority-spin (circles) $z$-even resonance $|n'\boldsymbol{k}\downarrow\rangle$, $\boldsymbol{k} = (0.05, 0.1)\pi/a_{2\mathrm{d}}$, $n' = 17$, with $\epsilon_{n'\downarrow}(\boldsymbol{k}) - \epsilon_{\mathrm{F}} = 0.0254$ eV (cf. figure 8 for $k_{||} = 0.112\pi/a_{2\mathrm{d}}$) in a (001) fcc Pd(11)/Co(16)/Pd(11) slab (i.e., for $p = 11$). The results are shown in one half of the slab only and are symmetrical in the other half.

degenerate at the $\overline{\Gamma}$ point and similar to the pairs of majority-spin QW states; see figure 8. At first sight, we do not observe a clear correlation between the energy position of these minority-spin state pairs and the oscillations of $K_1^{\downarrow\downarrow}$ with increasing $p$. However, when we plot, near the $\overline{\Gamma}$ point, the energies of those states that are localized mostly in the Pd overlayer we find that for $p = 5$ and $p = 11$ there exists a pair of such states with energies close to $\epsilon_F$, while there is no such pair for $p = 8$; see figure 8. This implies that the amplitudes of states belonging to a pair that is close to the Fermi energy $\epsilon_F$ are large in the Pd($p$) overlayer only for the same Pd thicknesses $p$ for which the majority-spin QW states cross $\epsilon_F$. These minority-spin states are pairs of *resonances* which largely resemble majority-spin QW states but differ from the latter in that they do not vanish completely in the Co layer; cf. figure 7. Thus, the pairs of the resonances appear periodically in the vicinity of the Fermi energy when the Pd thickness $p$ increases, and they are responsible for the oscillations of $K_1^{\downarrow\downarrow}$.

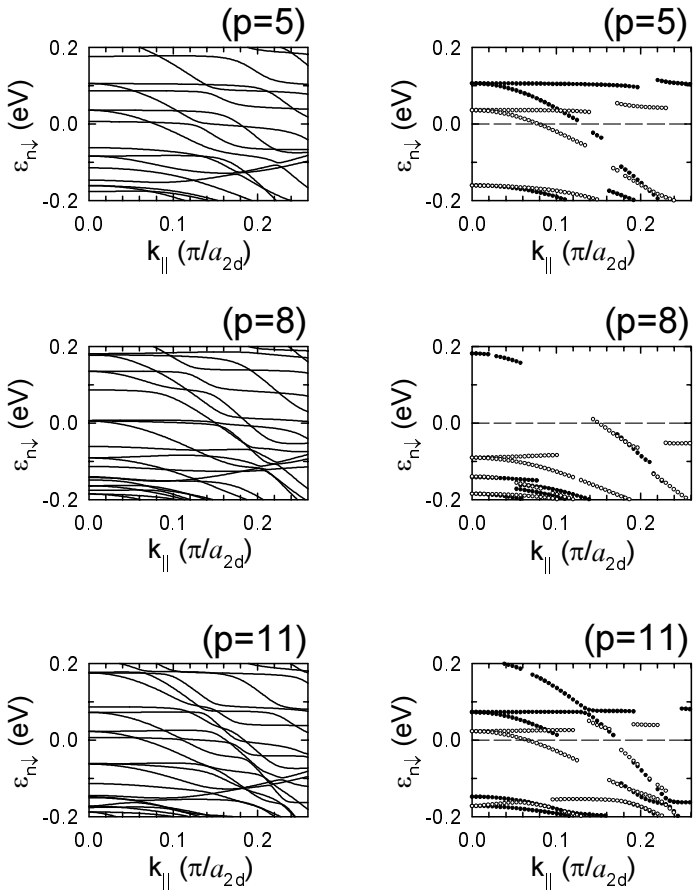


**Figure 8.** Energies of minority-spin (down-spin) electron states along the $k_y = 2k_x$ line near the $\overline{\Gamma}$ point in a (001) fcc Pd($p$)/Co(16)/Pd($p$) slab for different Pd thicknesses: $p = 5$, $p = 8$, and $p = 11$ (left column) and the corresponding *selected* energies of those $z$-even (○) and $z$-odd (●) minority-spin states $|n\boldsymbol{k}\downarrow\rangle$ whose average layer probability $|a_{\rm av}^{\rm Pd}|^2 = (1/p)\sum_{l=1}^{p}\sum_{\mu=1}^{5}|a_{n,l\mu}^{\downarrow}|^2$ in the Pd overlayer is at least *twice* larger than the average layer probability $|a_{\rm av}^{\rm Co}|^2 = (1/16)\sum_{l=p+1}^{p+16}\sum_{\mu=1}^{5}|a_{n,l\mu}^{\downarrow}|^2$ in the Co substrate (right column). The horizontal dashed line represents the Fermi energy $\epsilon_F = 0$.

*3.5. Semianalytical model for quantum-well states and resonances*

The majority-spin QW states and minority-spin resonances in question are mainly built of the $yz$ and $zx$ orbitals. This allows us to describe these states within a simplified TB model using $\mu = yz$ and $\mu = zx$ as the only basis orbitals.

For majority spin the amplitude $\boldsymbol{a}_l = (a_{lys}, a_{lzx})$ of the QW states vanishes in the cobalt part of the slab and the simplified TB equations in a Pd(p) overlayer take the form

$$\hat{V}_{\mathrm{Pd}}\boldsymbol{a}_1 + \hat{T}_{\mathrm{Pd}}\boldsymbol{a}_2 = \epsilon\,\boldsymbol{a}_1 \tag{14a}$$

$$\hat{T}^{+}_{\mathrm{Pd}}\boldsymbol{a}_{l-1} + \hat{V}_{\mathrm{Pd}}\boldsymbol{a}_l + \hat{T}_{\mathrm{Pd}}\boldsymbol{a}_{l+1} = \epsilon\,\boldsymbol{a}_l \qquad (l = 2, \ldots, p-1) \tag{14b}$$

$$\hat{T}^{+}_{\mathrm{Pd}}\boldsymbol{a}_{p-1} + \hat{V}_{\mathrm{Pd}}\boldsymbol{a}_p = \epsilon\,\boldsymbol{a}_p \tag{14c}$$

as for a free standing Pd slab. Here, $\hat{V}_{\mathrm{Pd}} = (V^{\mathrm{Pd}}_{\mu\nu}) = (H^{\sigma}_{l\mu,l\nu}(\boldsymbol{k}))$, $\hat{T}_{\mathrm{Pd}} = (T^{\mathrm{Pd}}_{\mu\nu}) = (H^{\sigma}_{l\mu,l+1\nu}(\boldsymbol{k}))$ where $\mu, \nu = yz, zx$ and $l, l+1$ are any two neighbouring Pd atomic layers. We take $\sigma = \uparrow$ but the matrices $\hat{V}_{\mathrm{Pd}}$, $\hat{T}_{\mathrm{Pd}}$ are the same for the opposite spin $\sigma = \downarrow$ in the paramagnetic Pd overlayer. The on-site potential matrix $\hat{V}_{\mathrm{Pd}}$ is assumed here to be layer-independent and hopping to farther than first-nearest-neighbours is neglected. For a (001) fcc slab, $\hat{T}_{\mathrm{Pd}}$ is real and $\hat{T}^{+}_{\mathrm{Pd}} = \hat{T}_{\mathrm{Pd}}$.

For an infinite fcc Pd crystal, equation (14*b*) holds for any $l$ and its real solutions

$$a_{l\mu} = b_\mu \sin \zeta l \tag{15}$$

are obtained by a linear combination of the Bloch functions $b_\mu e^{-i\zeta l}$ and $b_\mu e^{i\zeta l}$. Here, $\zeta = k_z a/2$ is proportional to the $z$-component (i.e., perpendicular to the layers) of a three-dimensional wave-vector $(\boldsymbol{k}, k_z)$. The amplitude $\boldsymbol{b} = (b_{yz}, b_{zx})$ of these bulk states fulfills the equation

$$\left[\hat{V}_{\mathrm{Pd}} + 2(\cos\zeta)\hat{T}_{\mathrm{Pd}}\right]\boldsymbol{b} = \epsilon\,\boldsymbol{b} \tag{16}$$

obtained from equation (14*b*). The two analytical solutions $\boldsymbol{b} = \boldsymbol{b}^{+}, \boldsymbol{b}^{-}$ of equation (16) and the corresponding energies $\epsilon = \epsilon^{+}_{\mathrm{b}}, \epsilon^{-}_{\mathrm{b}}$ are given explicitly in [12]. They depend both on $\zeta$ and $\boldsymbol{k}$. For $\boldsymbol{k} \in \Omega_\Gamma$ and $\zeta \lesssim \pi$, the solutions $\boldsymbol{b}^{\pm}(\boldsymbol{k}, \zeta)$ properly approximate true eigenstates in bulk Pd and seize to depend on $\zeta$ in the first approximation.

It is immediately seen that the bulk solution (15) is also valid for a finite slab described by equations (14) if $\zeta$ is chosen such that $\sin \zeta l = 0$ for $l = p+1$. Indeed, in such a case, we have $\boldsymbol{a}_{p+1} = \boldsymbol{a}_0 = 0$ so that equations (14*a*), (14*c*) are fulfilled once equation (14*b*) holds for any $l$. This leads to the quantization condition for the majority-spin QW states in the Pd overlayer:

$$\zeta = \zeta_m = \pi - \frac{m\pi}{p+1}, m = 1, 2, \ldots \tag{17}$$

here $m$ must be small ($m \ll p$) if $\zeta \lesssim \pi$. Thus, the analytical forms of majority-spin QW-states and their energies $\epsilon^{\pm}(\boldsymbol{k}) = \epsilon^{\pm}_{\mathrm{b}}(\boldsymbol{k}, \zeta_{\mathrm{F}})$, previously found in [12] in an approximate way, are now obtained in a strict manner, i.e., directly from the TB *slab* model.

The $m$th QW-state-pair energies $\epsilon^{+}_m$, $\epsilon^{-}_m$ move upwards when the Pd thickness $p$ grows and they cross the Fermi level $\epsilon_{\mathrm{F}}$ at $\boldsymbol{k} = 0$ when

$$p + 1 \approx \frac{m\pi}{\pi - \zeta_{\mathrm{F}}} = mL \tag{18}$$

where $\zeta_{\mathrm{F}}$ is such that $\epsilon^{\pm}_{\mathrm{b}}(0, \zeta_{\mathrm{F}}) = \epsilon_{\mathrm{F}}$. So, when $p$ increases, the Fermi level $\epsilon_{\mathrm{F}}$ is crossed by a QW state pair at regular intervals, i.e., periodically. The corresponding period $L = 5.67$ AL is determined by the magnitude of $\pi - \zeta_{\mathrm{F}}$ which is proportional to the extremal dimension of the Pd bulk Fermi surface in the $z$-direction [12]. This precise value of $L$, replacing the

approximate period of 6 AL deduced earlier from figure 1, is in perfect agreement with the period of 5.7 AL found in the *ab initio* calculations in [26]. Thus, we obtain from equation (18) the sequence of Pd thicknesses $p = 4.7, 10.3, 16.0, 21.7, \ldots$ coinciding almost exactly with the positions of the $K_1$ minima found in the full, five-d-band, TB calculations; cf. figure 1.

The simplified TB model (14) can be further enhanced to describe the minority-spin resonances. These states are assumed to have only $yz$- and $zx$-orbital components in the Pd overlayer and to spill out into the Co layer where, in principle, they can be composed of all five d-orbitals. Thus, for a Pd($p$)/Co($q$) slab the following TB equations

$$\hat{T}^{+}_{\mathrm{Pd}}\boldsymbol{a}_{p-1} + \hat{V}_{\mathrm{Pd}}\boldsymbol{a}_{p} + \hat{T}_{\mathrm{PdCo}}\tilde{\boldsymbol{a}}_{p+1} = \epsilon\,\boldsymbol{a}_{p} \tag{19a}$$

$$\hat{T}^{+}_{\mathrm{PdCo}}\boldsymbol{a}_{p} + \hat{V}_{\mathrm{Co}}\tilde{\boldsymbol{a}}_{p+1} + \hat{T}_{\mathrm{Co}}\tilde{\boldsymbol{a}}_{p+2} = \epsilon\,\tilde{\boldsymbol{a}}_{p+1} \tag{19b}$$

$$\hat{T}^{+}_{\mathrm{Co}}\tilde{\boldsymbol{a}}_{l-1} + \hat{V}_{\mathrm{Co}}\tilde{\boldsymbol{a}}_{l} + \hat{T}_{\mathrm{Co}}\tilde{\boldsymbol{a}}_{l+1} = \epsilon\,\tilde{\boldsymbol{a}}_{l} \qquad (l = p+2, \ldots, p+q-1) \tag{19c}$$

$$\hat{T}^{+}_{\mathrm{Co}}\tilde{\boldsymbol{a}}_{p+q-1} + \hat{V}_{\mathrm{Co}}\tilde{\boldsymbol{a}}_{p+q} = \epsilon\,\tilde{\boldsymbol{a}}_{p+q} \tag{19d}$$

hold in addition to equations (14$a$) and (14$b$). The amplitude $\tilde{\boldsymbol{a}}_l = (\tilde{a}_{l\mu})$ and the matrices $\hat{V}_{\mathrm{Co}} = (V^{\mathrm{Co}}_{\mu\nu}) = (H^{\downarrow}_{l\mu,l\nu}(\boldsymbol{k}))$, $\hat{T}_{\mathrm{Co}} = (T^{\mathrm{Co}}_{\mu\nu}) = (H^{\downarrow}_{l\mu,l+1\nu}(\boldsymbol{k}))$, with $p+1 \leqslant l \leqslant p+q$, $\mu$, $\nu = xy,\ yz,\ zx,\ x^2-y^2,\ 3z^2-r^2$, describe the Co part of the system. The interaction between the Pd and Co layers at the Co/Pd interface is included through the hopping matrix $\hat{T}_{\mathrm{PdCo}} = (T^{\mathrm{PdCo}}_{\mu\nu}) = (H^{\downarrow}_{p\mu,p+1\nu}(\boldsymbol{k}))$ (with $\mu = yz,\ zx$ and $\nu = xy,\ yz,\ zx,\ x^2-y^2,\ 3z^2-r^2$). As in equations (14), the hopping between first-nearest-neighbours is included only and the on-site potential matrices $\hat{V}_{\mathrm{Pd}}$ and $\hat{V}_{\mathrm{Co}}$ are assumed not to depend on the atomic layer index $l$ within the Pd and Co parts of the system, respectively. If we now assume, in a similar way to majority-spin electrons, that the eigenstates of minority-spin electrons are given in the Pd layer by the solution (15) with the energy $\epsilon = \epsilon(\zeta) = \epsilon^{+}_{\mathrm{b}}(\boldsymbol{k},\zeta)$ [or $\epsilon^{-}_{\mathrm{b}}(\boldsymbol{k},\zeta)$] then the TB equations (19$a$) and (19$b$) lead to the following relations:

$$\sin[(p+1)\zeta]\hat{T}_{\mathrm{Pd}}\boldsymbol{b} - \hat{T}_{\mathrm{PdCo}}\tilde{\boldsymbol{a}}_{p+1} = 0 \tag{20a}$$

$$\sin(\zeta p)\hat{T}^{+}_{\mathrm{PdCo}}\boldsymbol{b} + [\hat{V}_{\mathrm{Co}} - \epsilon_{\mathrm{b}}(\zeta)]\tilde{\boldsymbol{a}}_{p+1} + \hat{T}_{\mathrm{Co}}\tilde{\boldsymbol{a}}_{p+2} = 0. \tag{20b}$$

These two equations together with equations (19$c$) and (19$d$) form a set of $2+5q$ linear equations for $2+5q$ unknowns. Thus, non-zero solutions are subject to the requirement that the determinant of the $(2+5q)\times(2+5q)$ matrix corresponding to this set vanishes. This leads to an non-linear equation for $\zeta$ of the following general form:

$$F(\zeta) = \sin^2[(p+1)\zeta]\,f_1[\epsilon_{\mathrm{b}}(\zeta)] + \sin[(p+1)\zeta]\sin(p\zeta)\,f_2[\epsilon_{\mathrm{b}}(\zeta)] + \sin^2(p\zeta)\,f_3[\epsilon_{\mathrm{b}}(\zeta)] = 0. \tag{21}$$

It is immediately seen that the values $\zeta = \zeta_m$, obtained from the quantization condition (17) for majority-spin electrons, are very close to some of the exact solutions $\zeta$ of equation (21) valid for minority-spin electrons. Indeed,

$$F(\zeta = \zeta_m) = \sin^2\left[\frac{m\pi}{p+1}\right] f_3[\epsilon_{\mathrm{b}}(\zeta)] \tag{22}$$

is very small when $m \ll p$. Moreover, one can also argue that for a solution $\zeta \approx \zeta_m$ with $m \ll p$, when both $\sin(p\zeta) \approx 0$ and $\sin[(p+1)\zeta] \approx 0$, equations (20) imply that the amplitudes $\tilde{\boldsymbol{a}}_{p+1}$, $\tilde{\boldsymbol{a}}_{p+2}$, and, via equations (19$c$) and (19$d$), also all the remaining $\tilde{\boldsymbol{a}}_l$, should be significantly smaller than $\boldsymbol{b}$, and, in consequence, smaller than the amplitudes $\boldsymbol{a}_l$ in Pd layers. Thus, the minority-spin eigenstates with $\zeta \approx \zeta_m$ and energies $\epsilon = \epsilon^{\pm}_{\mathrm{b}}(\boldsymbol{k},\zeta) \approx \epsilon^{\pm}_{m}(\boldsymbol{k})$ are resonances, mostly confined in the Pd overlayer.

This explains why the minority-spin resonances appear at the Fermi level $\epsilon_F$ for the nearly same thicknesses of the Pd overlayer as the majority-spin QW states, i.e., periodically: with the same period $L = 5.67$ AL and in phase with the majority-spin QW states; cf. figure 8. According to the above analysis (cf. equation (22) in particular), such a situation takes place because the condition $\zeta = \zeta_m \lesssim \pi$, or equivalently $m \ll p$, is satisfied for electrons with $\boldsymbol{k} \approx 0$ and energies $\epsilon_b^{\pm}(\boldsymbol{k}, \zeta)$ close to $\epsilon_F$. This could only happen because the Fermi energy $\epsilon_F$ lies near the top of the d-band in bulk palladium.

### *3.6. Concluding remarks*

The findings of the previous section explain why all spin-pair contributions $K_1^{\sigma\sigma'}$ oscillate with the same period $L$ and in phase, and so does their sum, i.e., $K_1$. The oscillation amplitude of $K_1^{\downarrow\downarrow}$ is smaller than that of $K_1^{\uparrow\uparrow}$ because the amplitude $a_{n,l\mu}^{\downarrow}$ of a minority-spin resonance, contributing to the MA oscillations, is smaller in the Pd overlayer than the amplitude of $a_{n',l\mu}^{\uparrow}$ of the corresponding majority-spin QW state (cf. figure 7) while these amplitudes enter in the fourth power into the expression for the MA constant (see equation (5)). Obviously, the oscillation amplitude of $-K_1^{\uparrow\downarrow} = -K_1^{\downarrow\uparrow}$ should be between that of $K_1^{\downarrow\downarrow}$ and that of $K_1^{\uparrow\uparrow}$, just as found in figure 2 in [12].

The fact that the oscillation amplitudes of different contributions $K_1^{\sigma\sigma'}$ are not equal makes it possible that the sum of $K_1^{\sigma\sigma'}$, i.e., the total anisotropy constant $K_1$ oscillates with a non-zero amplitude. Indeed, for a *free-standing* Pd film, the contributions $K_1^{\sigma\sigma'}$ are also non-zero and oscillate as a function of the Pd film thickness with the same period as in the Co/Pd system investigated here, but the oscillations amplitudes of $K_1^{\uparrow\uparrow}$ and $K_1^{\downarrow\downarrow}$ are identical in this case and equal to the amplitudes of $-K_1^{\uparrow\downarrow} = -K_1^{\downarrow\uparrow}$. Thus, when the contributions $K_1^{\sigma\sigma'}$ are summed the resulting $K_1$ vanishes exactly and no MA oscillations are present. The different behaviour of the MA constant $K_1$ in the two systems compared here is ultimately due to the fact that electrons moving in a free-standing paramagnetic Pd film are subject to the same boundary conditions for both spins, while in a Pd overlayer put upon Co substrate the boundary conditions on the Co/Pd interface *depend* on the spin, especially for electrons with energies close to the Fermi level. Indeed, in this energy regime, only the minority-spin electrons can penetrate the Co substrate, while the electrons with the opposite, majority, spin are completely confined in the Pd overlayer. In this situation, the bulk-like states in the paramagnetic overlayer, which has no, or very small, magnetic moment of its own, can influence the MA energy which describes the dependence of the Co/Pd system energy on the direction of the system's magnetic moment originating in the ferromagnetic Co substrate layer. A similar argument [19, 20] based on the dependence of boundary conditions on electronic spin was used to explain the oscillations of the exchange coupling between two ferromagnetic layers separated by a paramagnetic layer of varying thickness.

The amplitudes $a_{n,l\mu}^{\sigma}$ of majority-spin QW states and minority-spin resonances oscillate in the Pd overlayer according to the formula (15). When the energies $\epsilon_m^{\pm} = \epsilon_b^{\pm}(\zeta_m)$ of these states cross the Fermi level $\epsilon_F$, so that $\zeta_m = \zeta_{m(\sigma,n)}$ is close to $\zeta_F$, the period of the amplitude oscillations

$$L_a \approx \frac{2\pi}{\zeta_F} = \frac{2}{1 - 1/L} \tag{23}$$

is close to 2 AL, as $\zeta_F \lesssim \pi$ or $1/L \ll 1$. On the other hand, the electron probabilities $|a_{n,l\mu}|^2 \sim \sin^2 \zeta_m l = \frac{1}{2}[1 - \cos 2(\pi - \zeta_m)l]$ oscillate in the Pd overlayer with the long period of around $\pi/(\pi - \zeta_F) = L = 5.67$ AL (cf. equation (18)) just as was found within the full, five-d-band, TB model; cf. figure 7. Similarly, the layer contributions $K_1^{(l)}$ depending on $l$ through the

quadratic terms $a^{\sigma}_{n_1,l\mu}[a^{\sigma}_{n_3,l\mu}]^* \sim (\sin \zeta_{m(\sigma,n_1)}l)(\sin \zeta_{m(\sigma,n_3)}l)$ (present in equation (8)) oscillate with a period close to $L = 5.67$ AL in the Pd part of the investigated systems. This explains why the same period of around 6 AL is found for both the oscillations of the total MA constant $K_1$ versus the Pd overlayer thickness $p$ (figure 1) and the oscillations of the layer contributions $K_1^{(l)}$ versus layer index $l$ in the Pd overlayer (figure 2).

According to Szunyogh and Györffy [27], the amplitude $A(p)$ of the MA oscillations behaves asymptotically as $p^{-2}$ at the zero temperature $T$. However, the MA oscillations reported here decay faster than $p^{-2}$, presumably due to the use of finite temperature $T$. In the analogy with the exchange coupling theory [20], it is expected that $A(p) \sim [p \sinh(ck_{\mathrm{B}}Tp)]^{-1}$ holds in the first approximation. A numerical fit for the present MA results seems to confirm this suggestion and the value of around $c = 4.5\ \mathrm{eV}^{-1}$ is found.

As shown in the present paper, the investigated MA oscillations in Co/Pd films come from QW states and corresponding resonances which originate in the vicinity of the $X$ point in the 3D BZ of bulk Pd and cross the Fermi level $\epsilon_{\mathrm{F}}$ as the Pd overlayer thickness increases. These QW states and resonances should not change significantly upon adding s and p orbitals in the TB model since, as the *ab initio* calculations [28] confirm, the bulk Pd states at and around the $X$ point are built almost entirely from d-orbitals. Also, since the present d-only TB model assumes the correct number (0.36 as given in [28]) of holes in the Fermi-surface hole pocket around $X$, the position of the Fermi level $\epsilon_{\mathrm{F}}$ with respect to the top of the Pd d band should remain almost unchanged if $\epsilon_{\mathrm{F}}$ was determined self-consistently in an more accurate TB model based on nine, s, p, d, orbitals. As this relative position of the Fermi level determines the MA oscillation period through equation (18), the MA energy should also oscillate with the same period of around 5.7 AL when s and p orbitals are included. These suppositions are supported by the results of the on-going work which aims to establish the effect of sp-d hybridization on MA in ultrathin magnetic films [29].

The QW states present in the Pd overlayer are responsible not only for the MA oscillations as shown in this paper, but also lead to the onset of magnetic moments in Pd layers which occur periodically when the Pd thickness grows. This effect, found theoretically for (001) fcc Ag/Pd systems in [26, 30], cannot be reproduced in the present d-only model where the layer magnetic moments have given, fixed, values and are not calculated self-consistently. However, the existence of small Pd moments, also present in the applied TB model (cf. [8]), is not an important factor in the MA oscillation problem because such moments do not alter significantly the Co/Pd-interface boundary conditions whose dependence on spin has been shown here to be the basic mechanism that allows the QW states to induce the non-zero MA oscillations. This conclusion is supported by the results of [12] where the majority-spin contribution to the MA oscillation was found to be well reproduced within the simplified two-band TB model assuming that the Pd overlayer is strictly paramagnetic.

## 4. Summary

The starting point of the present work was the numerical result of the MA oscillations versus the thickness of the paramagnetic Pd overlayer in Co/Pd slabs. The objective was to explain the internal mechanisms behind this unexpected theoretical finding. This goal has been achieved, with careful and detailed analysis, by tracing the origin of the MA oscillations down to individual electronic quantum states. The states responsible for the effect have turned out to be pairs of majority-spin quantum-well states and corresponding pairs of minority-spin resonances confined in the Pd overlayer (or partly confined in the case of resonances). These states appear near the Fermi level in the centre of the two-dimensional Brillouin zone. The results of the presented analysis give formal grounds for the simple approach used earlier [12] to explain the

period of the MA oscillations and to examine, in an approximate manner, the majority-spin contribution to these oscillations. The way that minority-spin electrons contribute to the MA oscillations is now also well understood. The present work provides a broad view on the investigated problem and gives a clear and solid proof of how the MA oscillations arise.

The techniques of analysis applied in the MA problem can also be used in the study of other physical quantities related to the electronic structure in systems of interest. This conclusion is particularly relevant to quantities expressed as a second-order correction in perturbed systems displaying two-dimensional translational symmetry. It should also be stressed that the presented methods of analysis, like the Pd-thickness-dependent $\boldsymbol{k}$-space MA breakdown, are not restricted to tight-binding models so that they can be used as well within *ab initio* approaches to electronic structure.

## Acknowledgments

I would like to acknowledge gratefully the support of the Engineering and Physical Sciences Research Council (UK) during my visits to Imperial College.

## References

[1] Chapert C, Le Dang K, Beauvillain P, Hurdequint H and Renard D 1986 *Phys. Rev.* B **34** 3192
[2] Johnson M T, de Vries J J, McGee N W E, aan de Stegge J and den Broeder F J A 1992 *Phys. Rev. Lett.* **69** 3575
[3] Lee J, Lauhoff G and Bland J A C 1997 *Phys. Rev.* B **56** R5728
[4] Gay J G and Richter R 1987 *J. Appl. Phys.* **61** 3362
[5] Kyuno K, Yamamoto R and Asano S 1993 *J. Magn. Magn. Mater.* **126** 268
[6] Cinal M, Edwards D M and Mathon J 1994 *Phys. Rev.* B **50** 3754
[7] Cinal M, Edwards D M and Mathon J 1995 *J. Magn. Magn. Mater.* **140–144** 681
[8] Cinal M and Edwards D M 1997 *Phys. Rev.* B **55** 3636
[9] Szunyogh L, Újfalussy B and Weinberger P 1995 *Phys. Rev.* B **51** 9552
[10] Újfalussy B, Szunyogh L and Weinberger P 1996 *Phys. Rev.* B **54** 9883
[11] Guo G Y 1999 *J. Phys.: Condens. Matter* **11** 4329
[12] Cinal M and Edwards D M 1998 *Phys. Rev.* B **57** 100
[13] Szunyogh L, Újfalussy B, Blaas C, Pustugova U, Sommers C and Weinberger P 1997 *Phys. Rev.* B **56** 14036
[14] Weber W, Bischof A, Allenspach R, Würsch Ch, Back C H and Pescia D 1996 *Phys. Rev. Lett.* **76** 3424
[15] Bounough A, Train C, Beauvillain P, Bruno P, Chappert C, Megy R and Veillet P 1997 *J. Magn. Magn. Mater.* **165** 484
[16] Engel B N, England C D, Van Leeuwen R A, Wiedmann M H and Falco C M 1991 *Phys. Rev. Lett.* **67** 1910
[17] Engel B N, England C D, Van Leeuwen R A, Nakada M and Falco C M 1991 *J. Appl. Phys.* **68** 5643
[18] Würsch Ch, Stamm C, Egger S, Pescia D, Baltensperger W and Helman J S 1997 *Nature* **389** 937
[19] Edwards D M, Mathon J, Muniz R B and Phan M S 1991 *Phys. Rev. Lett.* **67** 493
Edwards D M, Mathon J, Muniz R B and Phan M S 1991 *J. Phys.: Condens. Matter* **3** 4941
[20] Mathon J, Villeret M, Umerski A, Muniz R B, d'Albuquerque e Castro J and Edwards D M 1997 *Phys. Rev.* B **56** 11797
[21] Abate E and Asdente M 1965 *Phys. Rev.* **140** A1303
[22] Slater J C and Koster G F 1954 *Phys. Rev.* **94** 1498
[23] Andersen O K and Jepsen O 1977 *Physica* **91B** 317
[24] Pettifor D G 1977 *J. Phys. F: Metal Phys.* **7** 613
[25] Hartmann D, Weber W, Rampe A, Popovic S, and Güntherodt G 1993 *Phys. Rev.* B **48** 16837
[26] Niklasson A M N, Mirbt S, Skriver H L and Johansson B 1997 *Phys. Rev.* B **56** 3276
[27] Szunyogh L and Györffy B L 1999 *Phys. Rev. Lett.* **78** 3765
[28] Mueller F M, Freeman A J, Dimmock J O, Furdyna A M 1970 *Phys. Rev.* B **1** 4617
[29] Cinal M 2001 in preparation
[30] Mirbt S, Johansson B and Skriver H L 1996 *Phys. Rev.* B **53** R13310